

Supporting information for:

Cs₃Cu₄In₂Cl₁₃ Nanocrystals: A Perovskite-Related Structure with Inorganic Clusters at A sites

Roman Kaiukov^{†Δ}, Guilherme Almeida[†], Sergio Marras^Φ, Zhiya Dang[†], Dmitry Baranov,[†] Urko Petralanda[†], Ivan Infante^{†§*}, Enrico Mugnaioli[⊥], Andrea Griesi^{⊥□}, Luca De Trizio^{†*}, Mauro Gemmi^{⊥*}, Liberato Manna^{†*}

[†] Department of Nanochemistry, ^Φ Materials Characterization Facility, Istituto Italiano di Tecnologia, Via Morego 30, 16163 Genova, Italy

^Δ Dipartimento di Chimica e Chimica Industriale, Università degli Studi di Genova, Via Dodecaneso 31, 16146 Genova, Italy

[§] Department of Theoretical Chemistry, Faculty of Science, Vrije Universiteit Amsterdam, de Boelelaan 1083, 1081 HV Amsterdam, The Netherlands

[⊥] Center for Nanotechnology Innovation@NEST, Istituto Italiano di Tecnologia, Piazza San Silvestro, 12, 56127, Pisa, Italy

[□] Department of Chemistry, Life Sciences and Environmental Sustainability, University of Parma, Parco Area delle Scienze 17/A, Parma, 43124, Italy

Table S1. Results of the different elemental analyses performed on Cs-Cu-In-Cl NCs synthesized at 145°C

Technique	Atomic composition			
	Cs	Cu	In	Cl
EDS (SEM)	3.0	4.2	2.0	12.8
EDS (TEM)	2.7	4.3	2.0	9.4

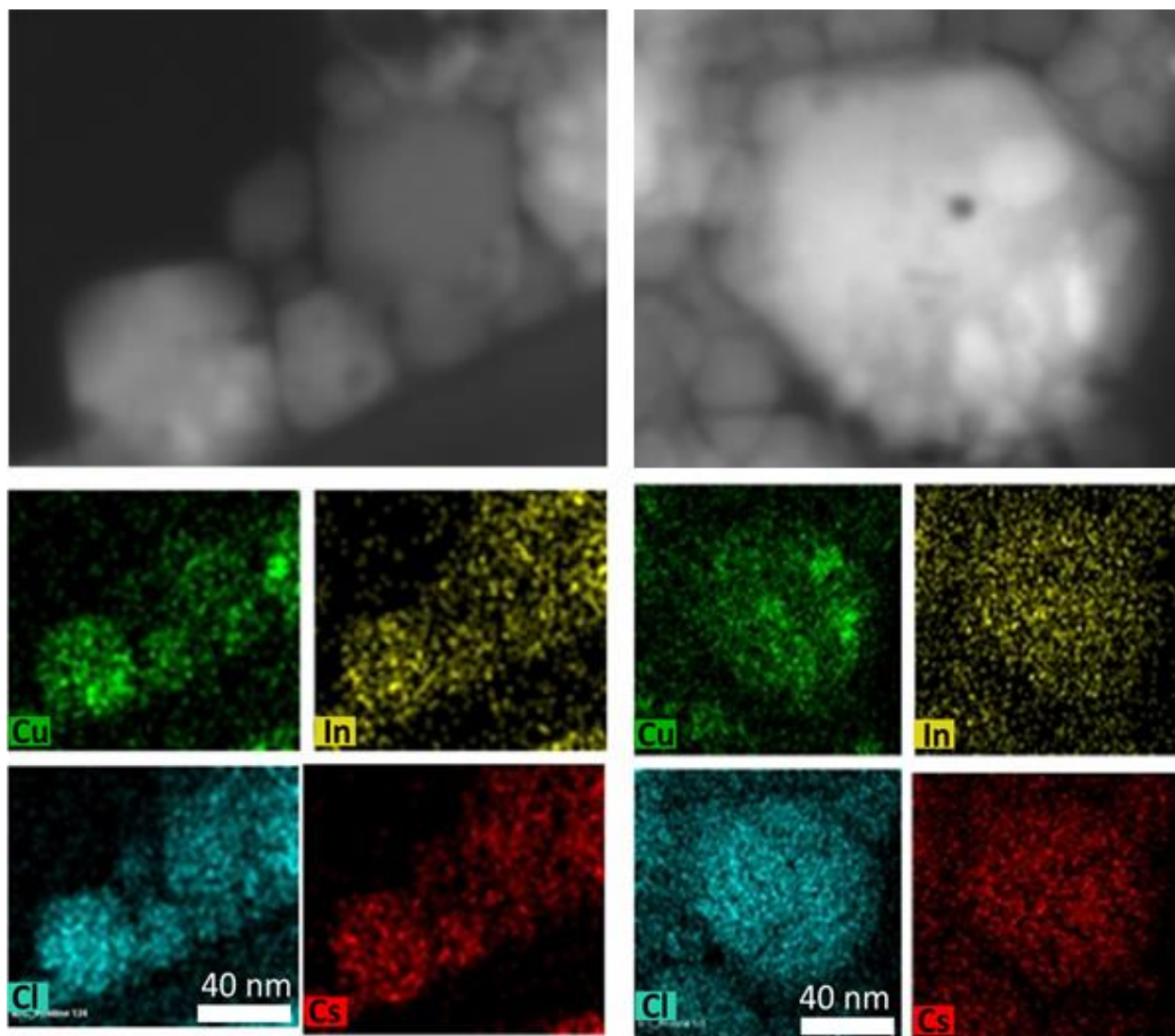


Figure S1. High-angle annular dark field micrographs and elemental maps for Cs, Cu, In and Cl.

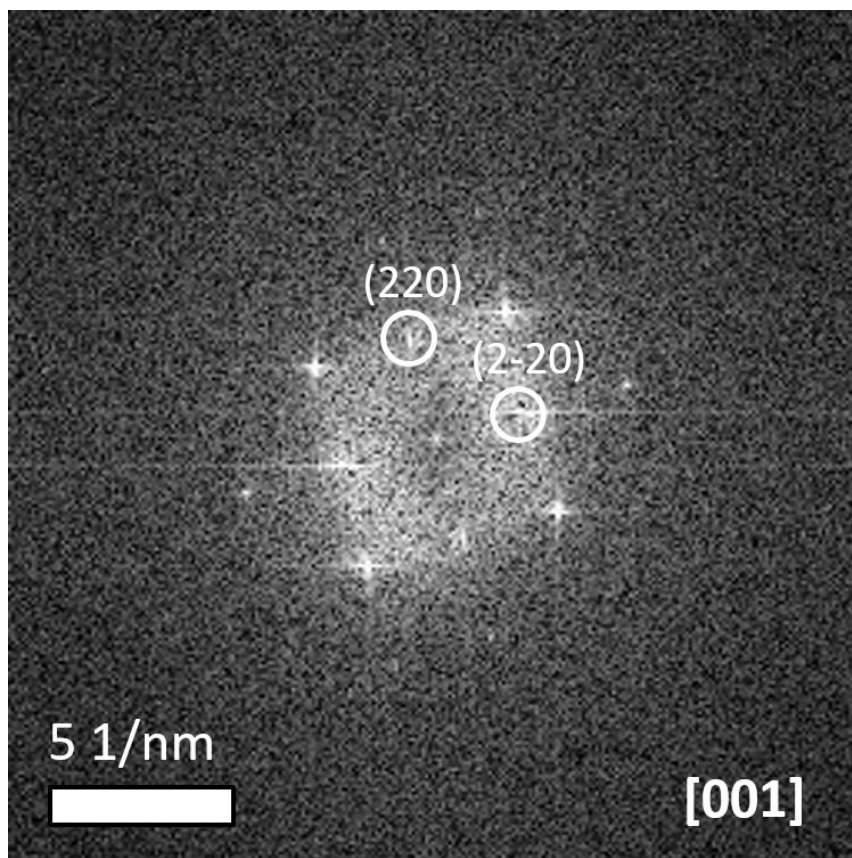


Figure S2. FFT image for the $\text{Cs}_3\text{Cu}_4\text{In}_2\text{Cl}_{13}$ NC shown in Figure 1b of the main text.

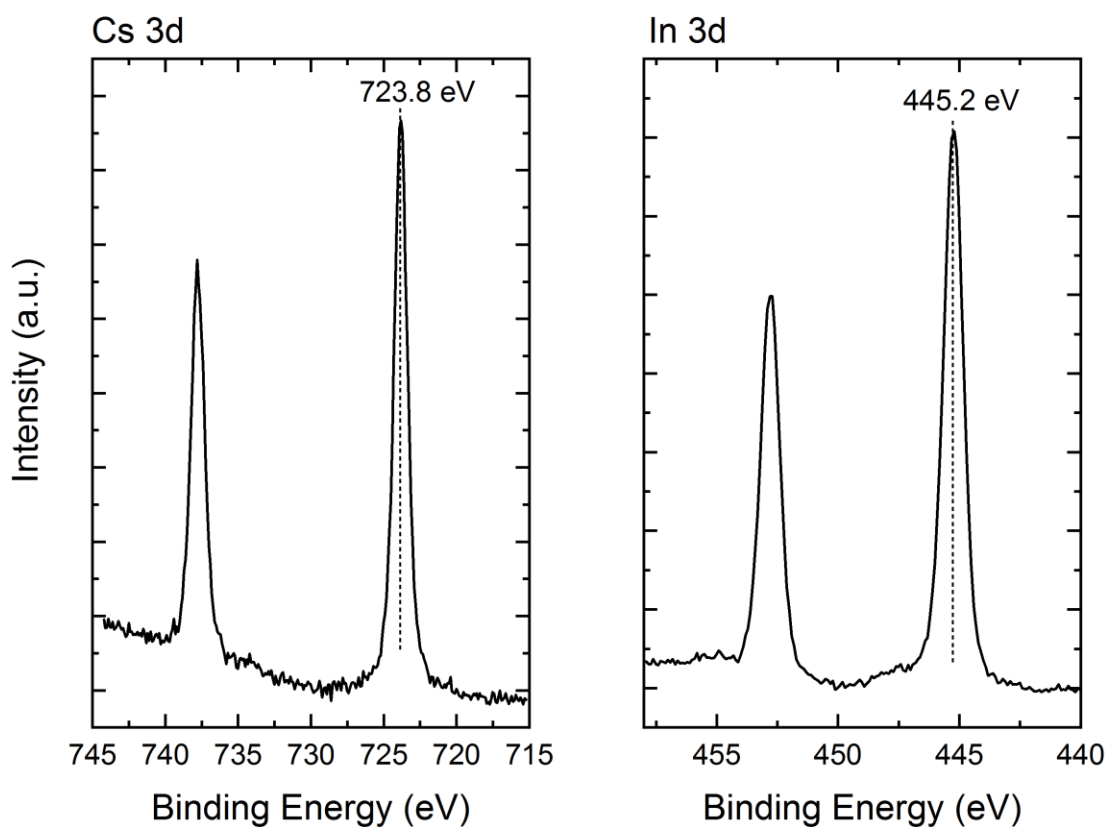


Figure S3. XPS spectra collected on a $\text{Cs}_3\text{Cu}_4\text{In}_2\text{Cl}_{13}$ NC sample. Data is shown over the binding energy ranges typical for Cs 3d and In 3d after calibration of the energy scale on the C 1s peak at 284.8 eV (adventitious carbon).

The observed peak positions, as reported in the panels, are consistent with the presence of Cs^+ and In^{3+} in agreement with data reported in [NIST X-ray Photoelectron Spectroscopy Database, Version 4.1 (National Institute of Standards and Technology, Gaithersburg, 2012); <http://srdata.nist.gov/xps/>] for the corresponding metal chlorides.

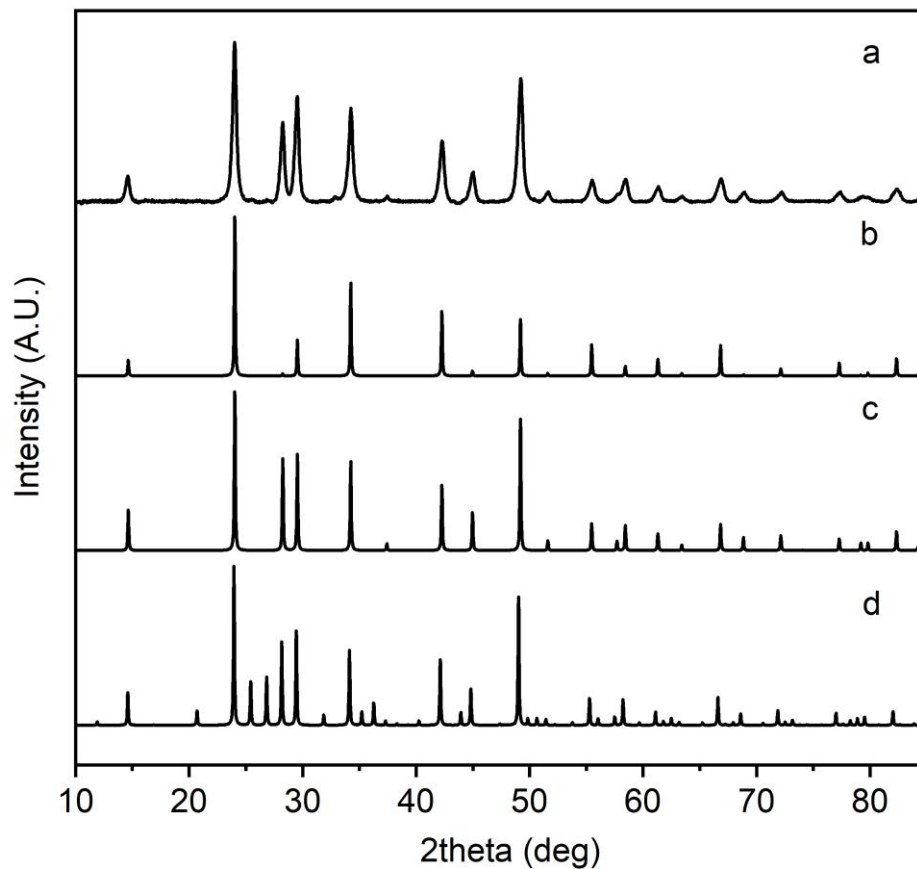


Figure S4. a) Experimental powder XRD pattern of the NCs synthesized at 145°C. b) Simulated powder XRD pattern of a $\text{Cs}_2\text{CuInCl}_6$ double perovskite (space group $Fm-3m$) structure, with lattice parameter equal to 10.48 Å. c) Rietveld refinement of the $Fm-3m$ disordered model of the $\text{Cs}_3\text{Cu}_4\text{In}_2\text{Cl}_{13}$ structure. d) Simulated powder XRD pattern from the primitive cubic $\text{Cs}_3\text{Cu}_4\text{In}_2\text{Cl}_{13}$ structure belonging to the $Pn-3m$ space group.

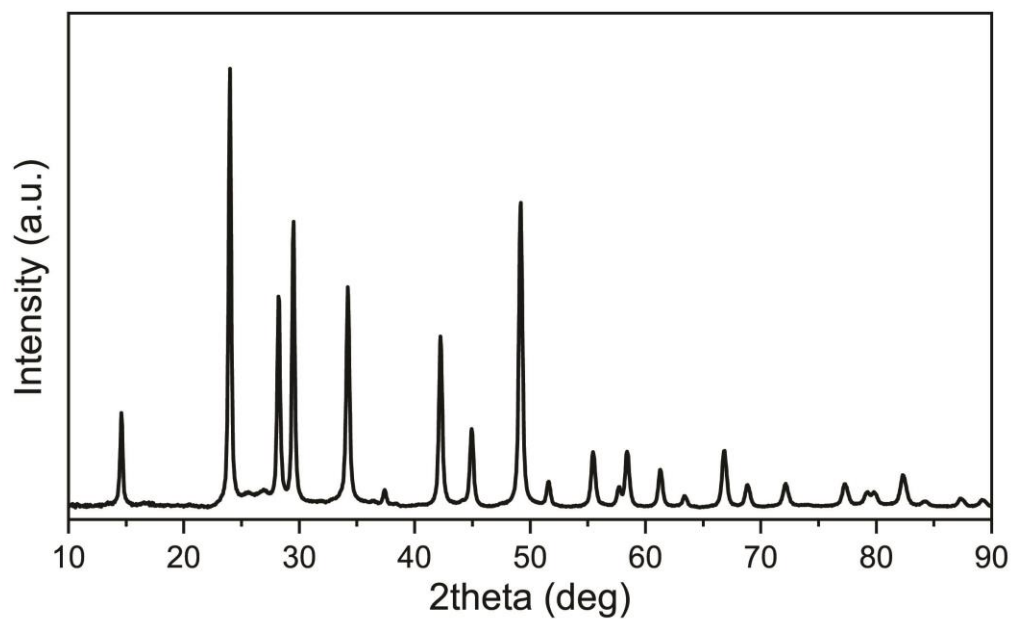


Figure S5. Powder XRD pattern of the NCs synthesized at 175°C specifically for the 3D-ED analysis. The pattern is almost identical to that of the sample synthesized at 145°C (Figure S4, “a” pattern), the only difference being that narrower peaks are observed in the current pattern, consistent with the presence of bigger crystals. The FWHM of the main peak at around $2\theta = 24^\circ$ is 0.25° , while for the same peak of the sample synthesized at 145°C the value is 0.39° .

Table S2. Results of the SEM-EDS analyses performed on Cs-Cu-In-Cl NCs synthesized at 175°C

Atomic composition			
Cs	Cu	In	Cl
2.8	3.8	2.0	13.8

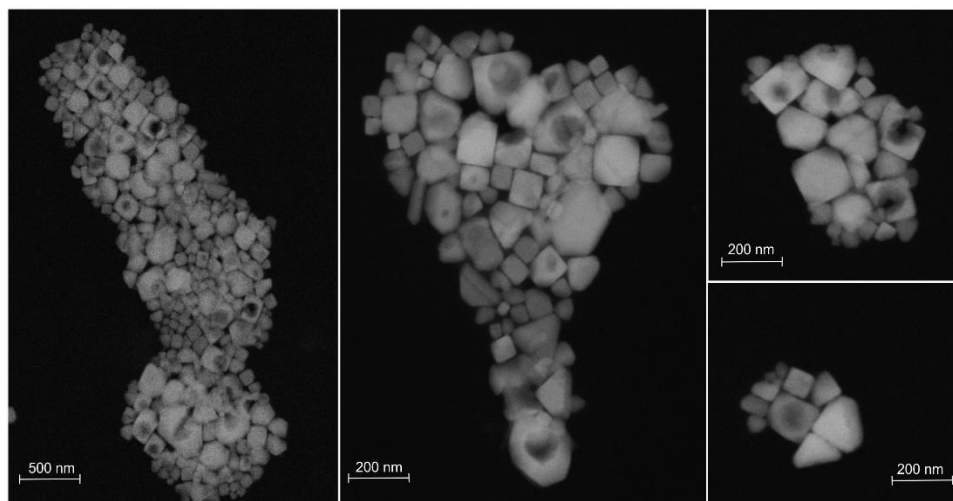


Figure S6. Exemplary dark-field STEM images of Cs-Cu-In-Cl NCs prepared for 3D ED measurements (synthesized at 175°C). Most NCs show cubic or triangular platelet habits, even if more irregular, intermediate shapes are also common.

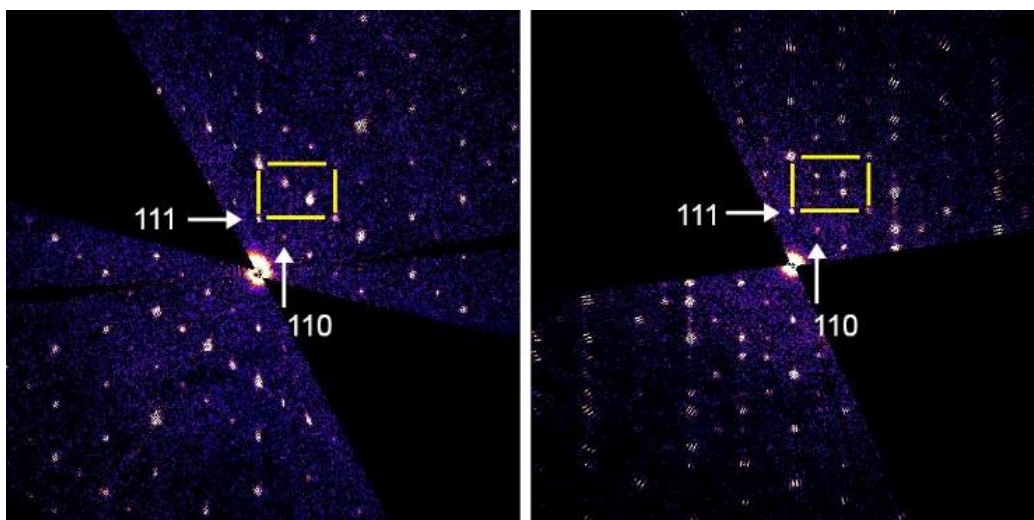


Figure S7. Section of the reciprocal space passing through the origin and parallel to the $[-110]$ reciprocal lattice plane of a single (left) and a twinned nanoparticle (right). The yellow rectangles with sides parallel to (111) and $(11-2)$ reciprocal directions are drawn as a guide for the eye for better noticing the doubling of spots parallel to (111) in the twinned nanoparticle.

Table S4. Experimental data and structural parameters on Cs-Cu-In-Cl NC structure solution and refinement by 3D ED.

Crystallographic details	
Unit cell content	Cs ₆ Cu ₈ In ₄ Cl ₂₆
Space group	<i>Pn-3m</i>
<i>a</i> , Å	10.5(2)
<i>b</i> , Å	10.5(2)
<i>c</i> , Å	10.5(2)
Cell volume, Å ³	1158(40)

3D ED data collection	
Mode	Continuous-rotation
Exposure, s	0.45
Tilt range, °	110
Tilt step, °	0.89

Ab initio structure determination in <i>Pnnn</i> (SIR2014)	
Data resolution, Å	0.9
N° sampled reflections	3675
N° independent reflections	785
Independent reflection coverage, %	93
<i>R</i> _{sym} , %	41.60
<i>R</i> _{SIR} , %	34.39

Least-squares refinement in <i>Pn-3m</i> (SHELXL)	
Data resolution, Å	0.9
N° reflections > 4σ	85
<i>R</i> _{int} , %	51.8
<i>R</i> 1 (4σ), %	32.95
<i>Goof</i>	2.512

Table S5. Rietveld refinement data

Total number of refined parameters: 31

Background model:

- Chebyshev polynomial: 16 coefficients

Experimental parameters:

- Gu, Gv, Gw parameters for the Gaussian profile of the pseudo- Voigt
- Lx, Ly parameters for the Lorentian profile of the pseudo- Voigt
- Zero shift
- Scale factor

Structural parameter:

- $a = 10.4670(3)$ Å

Atom	X	Y	Z	Occ.	Uiso
Cs1	0.25	0.25	0.25	0.7625(23)	0.0268(7)
In1	0.5	0.0	0.5	1.0	0.0119(9)
Cu1	0.8775(5)	0.1225(5)	0.3775(5)	0.2375(23)	0.0464(23)
Cl1	0.25	0.75	0.75	0.2375(23)	0.0268(7)
Cl2	0.74197(28)	0.0	0.5	1.0	0.0162(8)

Profile agreement factors:

- $R_p = 0.0241$
- $wR_p = 0.0326$

Structural agreement factor

- $R(F^2) = 0.0263$

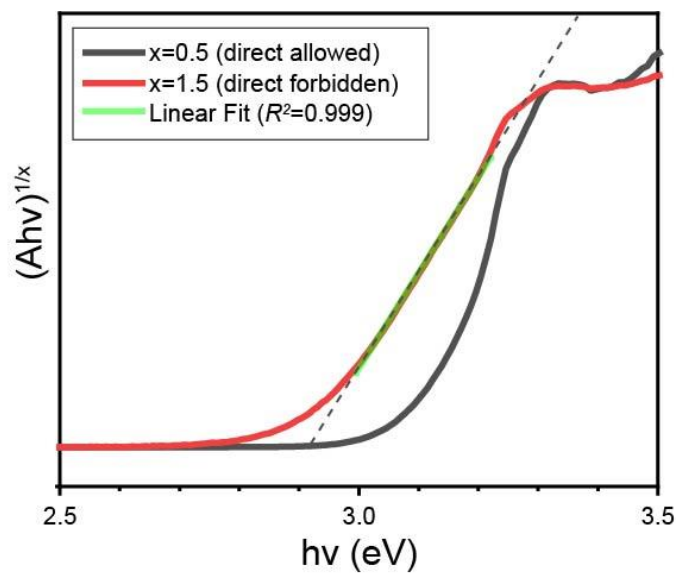


Figure S8. Tauc plot analysis of the absorbance spectrum considering direct allowed ($x = 0.5$) and direct forbidden ($x = 1.5$) bandgaps. The best linear fit ($y = 2.43x - 7.08$) was obtained for $x = 1.5$, with an estimated band gap of 2.91 eV.